ISNN:2181-1296

SHAROF RASHIDOV NOMIDAGI
SAMARQAND DAVLAT UNIVERSITETI

САМАРКАНДСКИЙ ГОСУДАРСТВЕННЫЙ
УНИВЕРСИТЕТ ИМЕНИ ШАРОФА РАШИДОВА

SAMARKAND STATE UNIVERSITY NAMED
AFTER SHAROF RASHIDOV

ILMIY AXBOROTNOMA

НАУЧНЫЙ ВЕСТНИК
SCIENTIFIC JOURNAL

ANIQ VA TABIIY FANLAR SERIYASI

Matematika, Mexanika, Informatika
Fizika, Kimyo, Biologiya, Geografiya

№ 1/2 (155)
2026

ISSN 2181-1296

ILMIY AXBOROTNOMA

НАУЧНЫЙ ВЕСТНИК SCIENTIFIC JOURNAL

2026-yil, 1-son (155/2) ANIQ VA TABIIY FANLAR SERIYASI

Matematika, Mexanika, Informatika, Fizika, Kimyo, Biologiya, Geografiya

Samarqand viloyat matbuot boshqarmasida ro‘yxatdan o‘tish tartibi 09-25.
Jurnal 1999-yildan chop qilina boshlagan va OAK ro‘yxatiga kiritilgan.

BOSH MUHARRIR **R. I. XALMURADOV, t.f.d., professor**
BOSH MUHARRIR O‘RINBOSARLARI: **H.A. XUSHVAQTOV, f-m.f.d., dotsent**

TAHRIRIYAT KENGASHI:

Sh.A.Alimov	- O‘zFA akademigi	**M.X.Ashurov**	- O‘zFA akademigi
S.N.Lakayev	- O‘zFA akademigi (SamDU)	**B.J.Axmedov**	- O‘zFA akademigi
M.M.Kamilov	- O‘zFA akademigi	**Q.G‘.G‘ulomov**	- O‘zFA akademigi
A.G.Yagola	- Moskva davlat universiteti professori (Rossiya)	**A.A.Zaxidov**	-Texas Nanotexnologiya instituti professori (AQSh)
Alberto Del Bimbo	-Florensiya universiteti professori (Italiya)	**N.B. Ferapontov**	- Moskva davlat universiteti professori (Rossiya)
Sh.Tugizov	-Kaliforniya universiteti professori (AQSh)	**V.L.Popov**	-Berlin texnika universiteti professori (Germaniya)
A.S.Soleev	- f.-m.f.d., professor (SamDU)	**N.F.Bunkin**	- Moskva davlat texnika universiteti professori (Rossiya)
I.A.Ikromov	- f.-m.f.d., professor (SamDU)	**Haji Akber Aisa**	-Xinjiang tibbiyot universiteti professori (Xitoy)
B.X.Xo‘jayarov	- f.-m.f.d., professor (SamDU)	**E. A. Abduraxmonov**	- k.f.d., professor (SamDU)
L.Sabirov	-f.-m.f.d., professor (SamDU)	**N. K. Muxamadiyev**	- k.f.d., professor (SamDU)
A.Jumaboyev	-f.-m.f.d., professor (SamDU)	**L. A. Bulavin**	- Kiev milliy universiteti
X.Bozorov	-k.f.d., professor (SamDU)	**X. Q. Xaydarov**	- b.f.d., professor (SamDU)
O.Q.Quvondiqov	-f.-m.f.d. professor (SamDU)	**Z. I. Izzatullayev**	- b.f.d., professor (SamDU)
A.Z.Xasanov	-f.-m.f.d. professor (SamDU)	**A.B.Hasanov**	-tex.f.d., professor (SamDU)
Muhammad Suzuri bin Hitam	- Terengganu universiteti professori (Malayziya)	**Sh. T. Xoliqulov**	- q.-x.f.d., professor (SamDU)
K.D.Kuliyev	- f.-m.f .n. professor (SamDU)	**S. B. Abbosov**	- g.f.d., professor (SamDU)
A.M.Xolxo‘jayev	-f.-m.f.d., professor (SamDU)	**M.E. Mo‘minov**	-f.-m.f.d., professor (SamDU)
J.Abdullayev	-f.-m.f.d., professor (SamDU)	**I.I.Jumanov**	-tex.f.d., professor (SamDU)
A.R.Axatov	-tex.f.d., professor (SamDU)	**N.S.Mamatov**	-tex.f.d., professor (TIQXMMI)
D.B.Xursanov	- g.f.f.d., dotsent (SamDU)	**A.Sh.Yarmuxamedov**	-f-m.f.n., dotsent (SamDU)
F.Nazarov	-tex.f.d., dotsent (SamDU)	**X.S.Xaydarov**	-f-m.f.n., dotsent (SamDU)

Obuna indeksi – yakka tartibdagi obunachilar uchun **- 5583,**
tashkilot, korxonalar uchun **- 5584**

M U N D A R I J A
C O N T E N T S

№	Maqola nomi	Article title	Bet/ page
1.	Yuqori chastotali II-turdagi radio portlash spektral kuzatuvlaridan foydalanib magnit maydon kuchini baholash **Pulatov D., Mirtoshev Z.**	Estimation Of The Coronal Magnetic Field Strength Using High-Frequency Type Ii Radio Burst Observations **Pulatov D., Mirtoshev Z.**	**5-11**
2.	Rayxon (OCIMUM) o‘simligi efir moyi kimyoviy tarkibiga iqlim omillarining ta’sirini GX–MS usulida tadqiq etish **Siddikova Y., Saifullaeva Sh., Mukhamadiyev A., N.Fazlieva, Nayimova B., Muhamadiyev N.**	Study of the influence of climate factors on the chemical composition of basil (ocimum) essential oil using the GH–MS method **Siddikova Y., Saifullaeva Sh., Mukhamadiev A., N.Fazlieva, Nayimova B., Muhamadiev N.**	**12-20**
3.	Bentonitni montmorillonit bilan boyitishning samarali usullari va termal ishlov berishning kation almashinuvi quvvatiga ta'siri **Mamadoliev I., Abdikamalova A., Ruzieva S.**	Effective methods for bentonite enrichment with montmorillonite and the impact of thermal treatment on cation exchange capacity **Mamadoliev I., Abdikamalova A., Ruzieva S.**	**21-28**
4.	$KPbBr_3$ asosidagi peroled tuzilmalarida zaryad tashish mexanizmlari va energetik sathlarning moslashuvi **Rahmonova M., Muxamadiyev N.**	Charge transport mechanisms and energy level alignment in $KPbBr_3$ -based peroled structures **Rahmonova M., Mukhamadiev N.**	**29-36**
5.	*N*-(4-(((7-Nitroxinazolin-4-il) amino) metil)fenil) siklogeksankarboksamid sintezi **Gaybullaev Sh., Takhirov Y., Chao Niu, Bozorov Kh.**	Synthesis of N-(4-(((7-nitroquinazolin-4-YL) amino) methyl) phenyl) cyclohexanecarboxamide **Gaybullaev Sh., Takhirov Y., Chao Niu, Bozorov Kh.**	**37-41**
6.	3-brom-pirido[2,3-*d*]pirimidinonlarning sintezi **Khushnazarov Z., Turgunov D., Bozorov Kh.**	synthesis of 3-bromo-pyrido[2,3-d]pyrimidinones **Khushnazarov Z., Turgunov D., Bozorov Kh.**	**42-46**
7.	Zarrachalar tezlatkichlarida materiallarning aktivatsiyasi va radiatsion xavflar **Temirov J., Khasanov Sh., Safarov A., Karimberganova Q.**	Material activation and radiological hazards in particle accelerators **Temirov J., Khasanov Sh., Safarov A., Karimberganova Q.**	**47-57**
8.	Geoinformatsion dasturlar yordamida demografik atlaslar yaratishning afzalliklariga nazar **Tukhtamishev Sh., Khudoyarova Sh., Shirinboyev D.**	Advantages of creating demographic atlases using geoinformation software **Tukhtamishev Sh., Khudoyarova Sh., Shirinboev D.**	**58-62**
9.	Siklopropilatsetilen asosida atsetilen spirtlari sintezi, ularning nazariy energetik xarakteristikalari va nadfoksidaza oqsili (7U8G) bilan molekulyar birikish tahlili **Ziyadullaev M.E., Nurmanov S.E., Buriev F.Kh., Abdukhalikov F.J.**	Synthesis of acetylenic alcohols based on cyclopropylacetylene, their theoretical energetic characterization, and molecular docking analysis with nadph oxidase (7U8G) protein **Ziyadullaev M.E., Nurmanov S.E., Buriev F.Kh., Abdukhalikov F.J.**	**63-71**
10.	Tetratsiklik tieno[3,2-*d*]pirimidinonlarning siklooksigenaza-2 ingibitorlari sifatida *in silico* tadqiqi **Nasrullaev A., Buronov A., Gaybullaev Sh., Bozorov Kh.**	In silico evaluation of tetracyclic thieno[3,2-d]pyrimidinones as potential cyclooxygenase-2 inhibitors **Nasrullaev A., Buronov A., Gaybullaev Sh., Bozorov Kh.**	**72-76**
11.	H3PO4, KOH va ZnCl2 yordamida olingan faollashtirilgan ko‘mirning morfologik va strukturaviy xususiyatlarining qiyosiy tahlili **Ergasheva D., Mukhamadiyev A., Mukhamadiyev N., Uzokov J.**	Comparative analysis of the morphological and structural properties of activated carbon prepared using H_3PO_4, KOH, and $ZnCl_2$ **Ergasheva D., Mukhamadiev A., Mukhamadiev N., Uzokov J.**	**77-81**
12.	CO_2 NI quyosh nuri ta’sirida samarali konversiyalashni ta’minlovchi g-C_3N_4/$CoNi_2S_4$ geterotuzilmali nanomateriallar sintezi va fizik-kimyoviy xossalari **Samiev A., Nizamov U.N., Mirzaev Sh., Ruzimuradov O., Nasimov A.**	Synthesis and physicochemical properties of γ-C3N4/CoNi2S4 heterostructured anomaterials providing efficient conversion of CO2 under the influence of sunlight **Samiev A., Nizamov U.N., Mirzaev Sh., Ruzimuradov O., Nasimov A.**	**82-87**

№	Maqola nomi	Article title	Bet/ page
13.	Atrof muhitdagi ammiak mikrokensentratsiyasini monigitori uchun gibrid perovskit $MA_xFA_{1-x}PbI_3$ fluoressent sensori tayyorlash **Eshmuradova G.B., Tashpulatov Kh.Sh., Khursandov J.M., Normuradov O.U., Norboyev Q.M., Toshpulatov D.T.**	Preparation of hybride perovskite $MA_xFA_{1-x}PbI_3$-fluorescent sensor for the monitoring of ammonia microconcentration in environment **Eshmuradova G.B., Tashpulatov Kh.Sh., Khursandov J.M., Normuradov O.U., Norboev Q.M., Toshpulatov D.T.**	**88-92**
14.	Al^{3+} bilan modifikatsiyalangan shpinel tuzilishga ega $Li_{1.33}Al_XMn_{1.67-X}O_4$ ($0 \leq x < 0.7$) tarkibli adsorbentlarning zol-gel sintezi va fizik-kimyoviy xossalari **Begimkulova Sh.A., Nematova Sh.Sh., Baxriev I.S., Mirzaev Sh.E., Ruzimuradov O.N., Nasimov A.M.**	Sol-gel synthesis and physicochemical properties of adsorbents consisting of Al^{3+} modified spinel structure $LI_{1.33}Al_XMn_{1.67-X}O_4$ ($0 \leq X < 0.7$) **Begimkulova Sh.A., Nematova Sh.Sh., Baxriev I.S., Mirzaev Sh.E., Ruzimuradov O.N., Nasimov A.M.**	**93-99**
15.	CdCr2Se4 va CuCr4Se4 magnitli yarimo‘tkazgichda magnit-optik effektlar **Dosmurodov G.**, **Kurbaniyazov A.**, **Boboqambarova G.**	Magneto-optical effects in the magnetic semiconductor CdCr2Se4 AND CuCr4Se4 **Dosmurodov G.**, **Kurbaniyazov A.**, **Bobokambarova G.**	**100-104**
16.	Sophora lehmanni va Cicer mogoltavikum o‘simliklari yer ustki qismilarining flavonoidlari **Gafurov A.Zh, Botirov E. Kh.**	Flavonoids of aerial parts of sophora lehmannii and cicer mogoltavicum **Gafurov A.Zh, Botirov E. Kh.**	**105-109**
17.	Buxoro viloyatining balneologik resurslari va ularning aholi salomatligini yaxshilashdagi ahamiyati **Zaynutdinova D.K., Nematova Kh. Kh.**	Balneological resources of the bukhara region and their significance in improving public health **Zaynutdinova D.K., Nematova Kh. Kh.**	**110-116**
18.	Tabiiy cho‘kuvchan gruntlarni polimer-kompozitsion eritmalar bilan inyeksion mustahkamlash texnologiyasini matematik rejalashtirish **Bakhriyev N.F., Kholiqulov O.O., Nurmatova R.K.**	Mathematical planning of injection strengthening technology of natural collapsible soils using polymer-composite solutions **Bakhriyev N.F., Kholikulov O.O., Nurmatova R.K.**	**117-125**
19.	Adgezion kontaktlarda ishqalanish koeffitsiyentiga geometrik parametrlar hamda tashqi yuk ta’sirining tahlili **Bekmamatova G., Xoliqulov O., Tojinorov M.**	Analysis of geometric parameters and external load on the friction coefficient in adhesive contacts **Bekmamatova G., Xolikulov O., Tojinorov M.**	**126-131**
20.	Markaziy Osiyo iqlim sharoitida sorbsion sovutgichlardan biogaz komplekslari bilan simbiozda foydalanish istiqbollari **Abdusamiyev F., Bahriev S., Sattarov S.**	Prospects for using sorption refrigerators in symbiosis with biogas complexes in the climatic conditions of Central Asia **Abdusamiev F., Bahriev S., Sattarov S.**	**132-136**
21.	Maple tizimida algebraik ko’pxilliklarni ratsional parametrlashining nazariy asoslari va kompyuterda amalga oshirilishi **Usmonova N.**	Theoretical foundations and computer implementation of rational parameterization of algebraic manifolds in the maple system **Usmonova N.**	**137-142**
22.	$Fe_5Ga_6Gd_2YZr$ ko‘p komponentli kristallining element tarkibi va tebranish xossalarini rentgen-fluoresans (XRF) va raman spektroskopiyasi yordamida tadqiq etish **Nasirova N., Fayziyev Sh., Saidov Q., Qaxorova Sh., Sharipov M., Djuraev D.**	Investigation of the elemental composition and vibrational properties of the multicomponent crystal Fe5Ga6Gd2YZr using X-RAY fluorescence (XRF) and raman spectroscopy **Nasirova N., Fayziyev Sh., Saidov Q., Qaxorova Sh., Sharipov M., Djuraev D.**	**143-152**
23.	Xofp tipidagi tenglamalar sistemasi uchun Koshi masalasi **Erkinova D. A.**, **Imomnazarov Kh. Kh.**	Cauchy problem for a Hopf-type system **Erkinova D. A.**, **Imomnazarov Kh. Kh.**	**153-157**
24.	Ar va HCl izotopologlari o‘rtasida hosil bo‘lgan komplekslarning kvant-kimyoviy tahlili: AIM, RDG va NCI usullari yordamida solvatatsiya effektlarini o‘rganish **Khujamov U.**	Quantum-chemical analysis of complexes formed between Ar and HCL isotopologues: studying solvation effects using AIM, RDG, and NCI methods **Khujamov U.**	**158-167**

UDC: 523.9 https://doi.org/10.59251/2181-3973.2025.v1.138.1.3767

ESTIMATION OF THE CORONAL MAGNETIC FIELD STRENGTH USING HIGH-FREQUENCY TYPE II RADIO BURST OBSERVATIONS

D.Pulatov, Z.Mirtoshev
Samarkand State Univesrsity named after Sharof Rashidov, Samarkand, Uzbekistan.

D.Pulatov Samarkand State University named after Sharof Rashidov, Samarkand, Uzbekistan.

Received: 16.01.2026
Revised: 27.01.2026
Accepted: 13.02.2026
Published: 30.03.2026

Publisher: Samarkand State University named after Sharof Rashidov.

Abstract. We report the estimation of the coronal magnetic field strength in the height range of 1.04–1.08 $R_\odot$ using radio observations of a high-frequency band-splitting type II radio burst associated with an X2.2 solar flare and a fast coronal mass ejection (CME) on 2024 December 8. The burst was recorded by the e-CALLISTO (Uzbekistan) radio spectrometer in the frequency range of 45–413 MHz. By analysing the band-splitting between the upper and lower frequency sub-bands of the split emission lane, we derived the upstream-to-downstream density jump X = 1.472–1.513 and the Alfvén Mach number Ma = 1.373–1.407, confirming a weakly super-Alfvenic shock. The coronal magnetic field strength is estimated to be 7.27–10.15 G, following a power-law $B = 13.32\ r^{-8.02}$ (in Gauss). The shock speed derived from height-time measurements (1192 km/s) exceeds the CME leading-edge speed (913 km/s), consistent with a CME-driven shock propagating through dense coronal loops in the inner corona. These results provide new observational constraints on the coronal magnetic field at very low heliocentric heights, demonstrating the scientific value of ground-based high-frequency radio monitoring.

Keywords: coronal mass ejection, MHD shock, type II radio burst, band-splitting, coronal magnetic field.

Yuqori chastotali II-turdagi radio portlash spektral kuzatuvlaridan foydalanib magnit maydon kuchini baholash

Annotatsiya. Ushbu ishda 2024-yil 8-dekabrda kuzatilgan X2.2 sinf quyosh chaqnashi va koronal massa tashlanmalari (KMT) bilan bog‘liq yuqori chastotali spektral-bo‘linishli II turdagi radio portlash kuzatuvlari asosida 1,04–1,08 $R_\odot$ geliotsentrik balandlik oralig‘ida koronal magnit maydon kuchlanganligini baholash natijalar keltirilgan. II turdagi radio portlash e-CALLISTO (O‘zbekiston) radiospektrometri tomonidan 45–413 MGts chastota diapazonida qayd etilgan. Fundamental va garmonik emissiya komponentlari o‘rtasidagi tasma bo‘linishini tahlil qilish orqali zichlik sakrashi X = 1,472–1,513 va Alfven Mach soni M_A = 1,373–1,407 aniqlanib, zarba to‘lqinining kuchsiz o‘ta-Alfven xususiyati tasdiqlandi. Koronal magnit maydon kuchlanganligi 7,27–10,15 G oralig‘ida baholandi va $B = 13,32\ r^{-8,02}$ (Gaussda) qonuniga bo‘ysunishi aniqlandi. Balandlik-vaqt o‘lchovlaridan olingan zarba to‘lqini tezligi (1192 km/s) KMT tezligidan (913 km/s) yuqori bo‘lib, bu KMT tomonidan boshqariladigan zarbali to‘lqinning ichki toj zich magnit maydon halqalari orqali tarqalishiga mos keladi. Olingan natijalar juda past geliosentrik balandliklarda koronal magnit maydon uchun yangi kuzatuv cheklovlarini ta‘minlaydi va yerga asoslangan yuqori chastotali radio kuzatuvlarining ilmiy ahamiyatini ko‘rsatadi.

Kalit so‘zlar. Koronal massa tashlanmalari, MHD zarba, II-tur radio portlash, spektral bo‘linish, magnit maydon.

Оценка напряжённости магнитного поля солнечной короны на основе наблюдений высокочастотных полосно-расщеплённых радиовсплесков II типа

Аннотация. В данной работе представлена оценка напряжённости магнитного поля солнечной короны в диапазоне гелиоцентрических высот 1,04–1,08 $R_\odot$ на основе радионаблюдений высокочастотного полосно-расщеплённого радиовсплеска II типа, связанного со вспышкой класса X2.2 и быстрым корональным выбросом массы (КВМ) 8 декабря 2024 года. Всплеск был зарегистрирован радиоспектрометром e-CALLISTO (Узбекистан) в диапазоне частот 45–413 МГц. По результатам анализа полосного расщепления между фундаментальной и гармонической компонентами излучения определён скачок плотности X = 1,472–1,513 и число Альфвена-Маха M_A=1,373–1,407, что подтверждает слабо сверхальфвеновский характер ударной волны. Напряжённость магнитного поля короны оценена в диапазоне 7,27–10,15 Г и описывается степенным законом B = 13,32 $r^{-8,02}$ (в Гауссах). Скорость ударной волны по данным высотно-временных измерений (1192 км/с) превышает скорость переднего края КВМ (913 км/с), что соответствует модели поршневой ударной волны, распространяющейся через плотные корональные петли во внутренней короне. Полученные результаты обеспечивают новые наблюдательные ограничения на магнитное поле короны на очень малых гелиоцентрических высотах и демонстрируют научную ценность наземного высокочастотного радиомониторинга.

Ключевые слова. сорональными выбросами массы, ударная волна, солнечное излучение, магнитное поле

Introduction. Type II bursts are produced by magnetohydrodynamic (MHD) shock waves, typically driven by CMEs, which accelerate electrons to suprathermal energies [13]. These accelerated electrons excite Langmuir waves, which are subsequently converted into electromagnetic radiation, manifesting as fundamental and harmonic emission bands in the dynamic spectrum [4, 5]. The observed band-splitting phenomenon between the fundamental and harmonic components is widely interpreted as a consequence of density variations and upstream–downstream plasma structures within the shock region [15]. In most cases, type II burst starting frequencies are below 150 MHz, although in some cases they occur at higher frequencies [8, 11].

High-frequency type II radio bursts are generally generated in the low solar corona at heliocentric distances of $r < 1.5\ R_\odot$. According to [15], high-frequency type II bursts are primarily associated with solar flares, whereas low-frequency type II bursts are more frequently related to coronal mass ejections (CMEs). The fundamental emission component of high-frequency type II bursts typically does not exceed a few hundred MHz and exhibits a strongly impulsive profile. A statistical study by [1] demonstrated that most high-frequency type II bursts originate in the lower corona and are predominantly driven by flare-related processes. Their onset times were found to coincide closely with the impulsive phase of the associated flares, indicating a strong temporal and physical relationship. Furthermore, [6] reported that high-frequency (≈300 MHz) type II bursts observed in the inner corona at heights of approximately 1.4 $R_\odot$ were closely associated with shock formation. They also estimated that the coronal magnetic field strength ranged from about 1.3 G to 1.5 G at heliocentric distances between 1.2 $R_\odot$ and 1.5 $R_\odot$. [6] studied the relationship between occurred on 13 February 2011 high-frequency (drift rate 2.5 MHz/s) type II bursts and CMEs. They used SDO/AIA density models to determine the distance between the shock and the leading edge of the CME. They concluded that high-frequency type II bursts are generated in the lower corona by a CME shock that passes through high-density loops. [9] studied high-frequency type II bursts produced by

shocks with a drift rate of 2 MHz/s and a maximum speed of 2500 km/s. They found a correlation between the shock speed profile obtained from radio observations and the associated soft X-ray flare light curve. They also confirmed that high-frequency type II bursts originate from MHD shock driven by CMEs. In a statistical study [14], 40 high-frequency type II bursts recorded between 2010 and 2016 were correlated with CME properties. They found that the heliocentric distance of the CME from 1.16 $R_\odot$ to 1.9 $R_\odot$ during the onset time of high-frequency type II bursts.

In this work, we characterize the magnetic field strength in the height range of 1.04–1.08 $R_\odot$ using radio observations of a high-frequency type II burst. We compare the shock speed derived from radio drift rate measurements with the CME leading-edge speed derived from LASCO height-time measurements. This work will be of great importance in studying the kinematics of CMEs very close to the solar surface.

Observation. The high-frequency type II radio burst was observed by the Compound Astronomical Low frequency Low-cost Instrument for **S**pectroscopy and **T**ransportable **O**bservatory (CALLISTO) Uzbekistan radio spectrometer, which covers the frequency range of 45–413 MHz. The burst was associated with an X2.2 class solar flare from active region AR 13912 located near the solar limb (S08W53). The flare started at 08:50 UT, peaked at 09:06 UT, and ended at 09:10 UT as recorded in the GOES 1–8 Å soft X-ray channel.

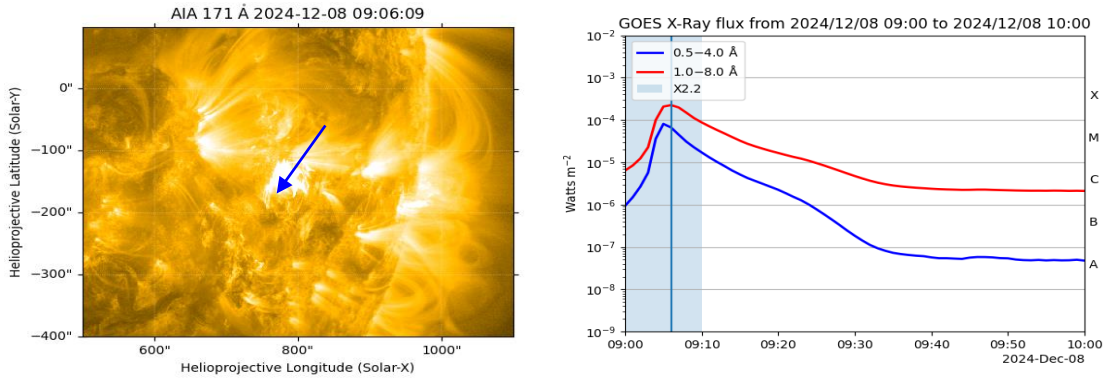

Figure 1. (left) SDO / AIA 171 Å filter observation after the high frequency type II burst. The (right) image shows the GOES X-ray flux curves for solar flare. Vertical line shows peak value of solar flare intensity. GOES observed the flare in two energy bands: 1 – 8 Å (red line) and 0.5 – 4 Å (blue line).

The early-phase eruption of the CME is visible in SDO/AIA 171 Å images (Figure 1), which show the expanding structure in the low corona at heliocentric distances of approximately 1.0–1.5 $R_\odot$. The type II radio burst exhibits a clear band-splitting structure, with both fundamental (F) and harmonic (H) emission components visible in the dynamic spectrum. The band-splitting was measured during the interval 09:05:55–09:06:45 UT, coinciding with the peak of the associated X-ray flare. The observed drift rate of the fundamental component follows a power-law dependence on frequency, consistent with a decelerating shock propagating through the low solar corona.

Figure 2 (left panel) shows the dynamic spectrum recorded by the e-CALLISTO (Uzbekistan) radio spectrometer from 09:00 to 09:15 UT. The type II radio burst exhibits band-splitting, with both fundamental (F) and harmonic (H) emission lanes. The fundamental component shows a well-defined frequency drift. Following the type II burst, both type III and type IV radio emissions are visible in the spectrum. The right panel of Figure 2 shows a strong correlation (cc=0.94) between drift rate and low frequency, giving drift rate between 1.31 and 1.86 MHz/s in the band-splitting. This suggests that the CME-driven shock is being released at high speed from dense coronal loops in the low corona.

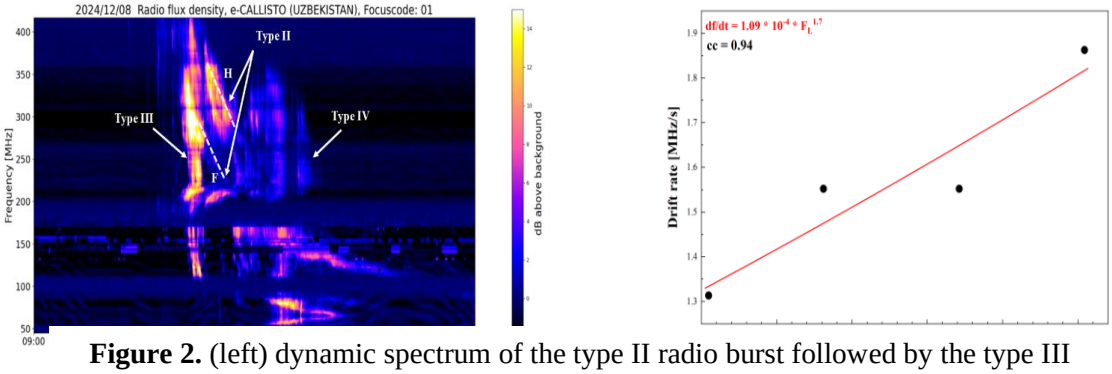

Figure 2. (left) dynamic spectrum of the type II radio burst followed by the type III and type IV moving burst observed by e-CALLISTO (Uzbekistan) radio spectrometer from 09:00 to 09:15 UT on 2024 December 8. F and H denoted harmonic and fundamental component of the high frequency type II radio burst. The (right) shows the drift rate is a distinct power law function of the frequency.

The shock speeds derived from the radio observation range from 797 to 908 km/s. A CME associated with this event was recorded by the Large Angle Spectroscopic cOronagraph (LASCO) and tracked using height-time measurements. The shock speed derived from height-time measurements is 1192 km/s (Figure 3a), while the CME speed was determined to be 913 km/s (Figure 3b). The difference between these two speeds indicates that the CME-driven shock propagates ahead of the CME leading edge through the ambient coronal plasma.

Results. The band-splitting of the observed high-frequency type II burst was used to derive the upstream-to-downstream density jump $X = (f_H/f_F)^2$, where f_H and f_F are the upper and lower frequency sub-bands of the split emission lane, respectively [15]. As shown in Figure 4a, the density jump X ranged from 1.472 to 1.487 during the interval 09:05:56–09:06:45 UT, reaching a peak value of ~1.513 at 09:06:18 UT. The corresponding Alfvén Mach number M_A varied between 1.373 and 1.407, peaking simultaneously with the density jump. Both quantities follow the same temporal trend, rising steeply from 09:05:56 UT and then declining after the peak at ~09:06:18 UT, reflecting the evolution of the shock strength as it propagates outward through the corona.

Figure 4b shows the temporal profiles of the shock speed V_{shock} and the local Alfvén speed V_A during 09:05:55–09:06:30 UT. The shock speed (from drift rate) ranges from ~797 to ~908 km/s, while the Alfvén speed ranges from ~568 to ~661 km/s. Both speeds follow a similar polynomial trend, declining from their initial values near 09:05:55 UT to a minimum at ~09:06:05 UT, then recovering to a secondary peak near 09:06:18–09:06:20 UT before declining again. Throughout the entire observation period, V_{shock} consistently exceeds V_A, confirming super-Alfvenic propagation of the shock. The average shock speed determined from the height-time measurements is 1192 km/s, while the CME leading-edge speed is 913 km/s, indicating that the shock propagates approximately 279 km/s faster than the CME driver.

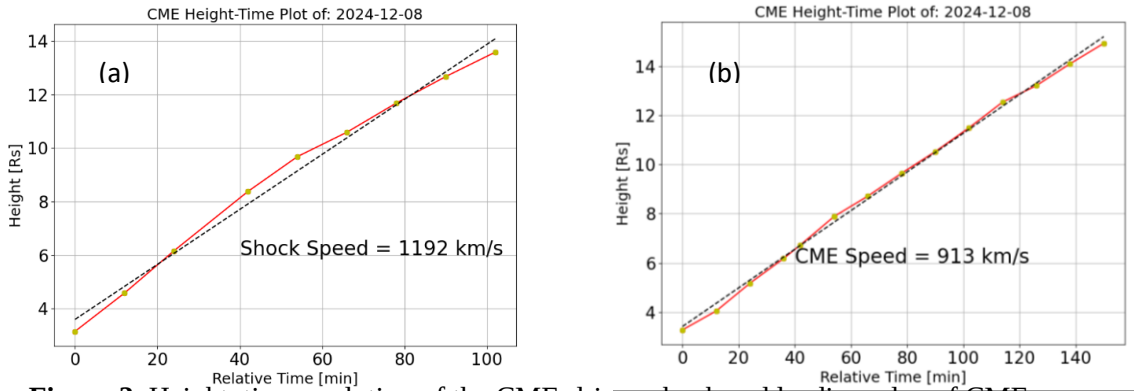

Figure 3. Height–time evolution of the CME-driven shock and leading edge of CME on 2024 December 8. First appearance of CME at 09:24 UT by C2 coronagraph. (a) Shock propagation with an estimated speed of 1192 km/s. (b) CME leading edge propagation with a speed of 913 km/s derived from LASCO C2 and C3 observations.

The coronal magnetic field strength B was estimated from the Alfvén speed and the local plasma density derived from the electron density model. We adopt the 1.8× Newkirk electron density model [12], which is widely used for active-region coronal plasma near the solar surface and was applied in comparable studies [6, 10].

Figure 5 shows the resulting B values as a function of heliocentric height, along with power-law fits from the present study and published results from [2, 5, 8, 9]. Our measurements yield B values in the range of 7.27–10.15 G at heliocentric heights of 1.04–1.08 $R_\odot$. The best-fit power-law for the present data gives $B = 13.32\ r^{-8.02}$ (in Gauss, with r in $R_\odot$), reflecting a steep decline of the magnetic field with height in the very low corona.

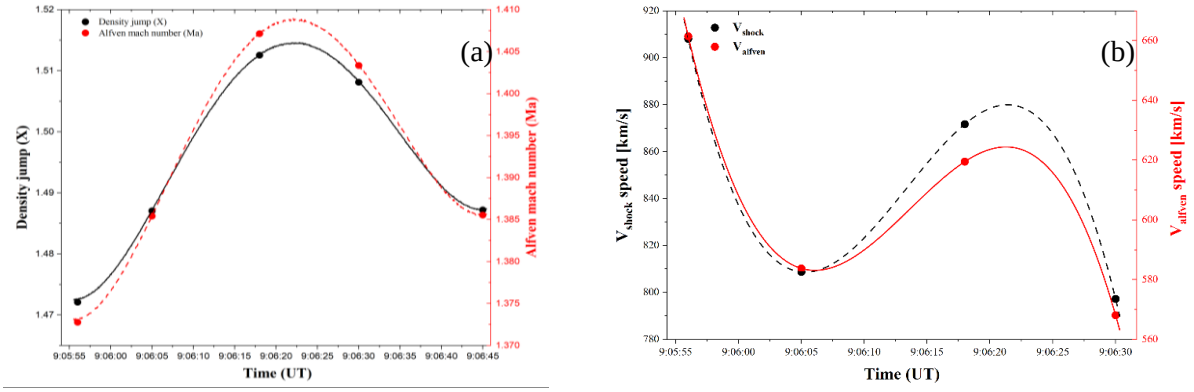

Figure 4. Temporal evolution of shock parameters during the 2024 December 8 type II radio burst. **(a)** Density jump X (black circles, left axis) and Alfven Mach number Ma (red circles, right axis) derived from band-splitting analysis during 09:05:55–09:06:45 UT. Both quantities peak simultaneously at ~09:06:20 UT. **(b)** Shock speed V_{shock} (black circles, left axis) determined from the radio observation and local Alfven speed V_{alfven} (red circles, right axis) during the same interval. The shock speed consistently exceeds the Alfven speed, confirming super-Alfvenic

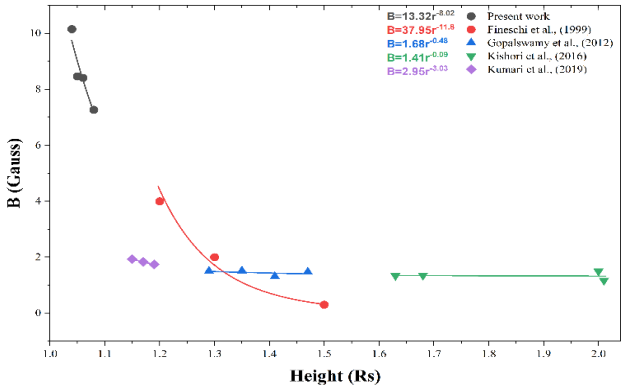

Figure 5. Coronal magnetic field strength as a function of heliocentric height. Black circles represent the present work ($B = 13.32\ r^{-8.02}$) derived from the 2024 December 8 high-frequency type II burst at heights 1.04–1.08 $R_\odot$. Solid lines show power-law fits from [3] red circles, [6] blue triangles, [7] green inverted triangles and [10] purple diamonds. Our measurements probe lower heights than most previous radio-based estimates, yielding stronger field values and a steeper radial gradient.

Discussion. The magnetic field values of 7.27–10.15 G obtained at heights of 1.04–1.08 $R_\odot$ are significantly higher than the estimates reported by [10], who found B values of 1.3–1.5 G at heliocentric distances of 1.2–1.5 $R_\odot$. This discrepancy is physically expected, given the steep radial decrease of the coronal magnetic field. Our measurements probe an altitude range closer to the solar surface than most previous radio-based studies, and the obtained power-law index of −8.02 is

considerably steeper than, for example, the index of −11.8 from [3] and −0.48 from [6], reflecting the sharp gradient of the field in the innermost corona. This positioning is physically consistent: our observations sample lower heights than [6], where the field is falling more steeply, yet the index is shallower than the [3] value, likely because that study targeted a different coronal structure. The differences among power-law indices from various studies can also be attributed to the different height ranges sampled, different density models employed, and the inherent variability of coronal magnetic field structures from event to event.

The Alfvén Mach number values (M_A ~ 1.373–1.407) indicate a weakly super-Alfvenic shock, consistent with other observations of high-frequency type II bursts generated in the low corona [9, 14]. The relatively low Mach number, combined with the high shock speed of 1192 km/s, implies a correspondingly high Alfvén speed in the source region, which is further evidence for strong magnetic fields near the solar surface. The excess speed of the shock over the CME leading edge (~279 km/s) is in good agreement with predictions from MHD shock theory, confirming that the CME acts as a driver for the coronal shock at very low heights. This is consistent with the conclusions of [2] and [9], who demonstrated that high-frequency type II bursts are produced by CME-driven shocks propagating through dense coronal loops in the low corona.

The temporal variation of the density jump and Alfven Mach number (Figure 4 a,b) reveals that shock strength is not constant but evolves as the shock traverses the low corona. The peak in both parameters near 09:06:20 UT may reflect the shock encountering a region of enhanced coronal density or a current sheet structure, temporarily increasing the density contrast across the shock front. This type of structured coronal interaction has been reported in previous studies [15] and underscores the importance of high-resolution radio observations for resolving fine temporal structure in the shock evolution.

Conclusion. In this study, we have estimated the coronal magnetic field strength in the height range of 1.04–1.08 $R_\odot$ using radio observations of a high-frequency band-split type II radio burst associated with an X2.2 flare and a fast CME. The key findings of this work are as follows. The coronal magnetic field strength in the height range 1.04–1.08 $R_\odot$ is estimated to be approximately 7.27–10.15 G, with a power-law dependence $B = 13.32\ r^{-8.02}$, indicating a steep radial field gradient in the innermost corona. The band-splitting analysis yields an upstream-to-downstream density jump X in the range 1.472–1.513 and a corresponding Alfvén Mach number M_A = 1.373–1.407, confirming a weakly super-Alfvenic shock. The shock speed derived from height-time measurement (1192 km/s) exceeds the CME leading-edge speed (913 km/s), demonstrating that the shock propagates ahead of its CME driver and is consistent with MHD shock theory. Both the shock speed and the Alfvén speed exhibit clear temporal variability during the event, likely reflecting structured density and magnetic field inhomogeneities in the low corona. These results extend the known measurements of the coronal magnetic field to very low heliocentric heights and demonstrate the capability of high-frequency type II burst observations from ground-based instruments such as e-CALLISTO to probe the innermost coronal environment. In the future, a statistical survey of high-frequency type II bursts recorded by e-CALLISTO during Solar Cycle 25 could systematically map the coronal magnetic field below 1.1 $R_\odot$, providing the broad observational baseline needed to improvement MHD shock models and CME initiation theories in the innermost corona.

References

1. Cane, H.V. and Reames, D.V., 1988. Some statistics of solar radio bursts of spectral types II and IV. Astrophysical Journal, Part 1 (ISSN 0004-637X), vol. 325, Feb. 15, 1988, p. 901-904., 325, pp.901-904, https://doi.org/10.1086/166061.

2. Cho, K.S., Gopalswamy, N., Kwon, R.Y., Kim, R.S. and Yashiro, S., 2013. A high-frequency type II solar radio burst associated with the 2011 February 13 coronal mass ejection. The Astrophysical Journal, 765(2), p.148, https://doi.org/10.1088/0004-637X/765/2/148.
3. Fineschi, S., van Ballegoijen, A. and Kohl, J.L., 1999, October. Coronal magnetic field diagnostics with UV spectropolarimeter. In 8th SOHO Workshop: Plasma Dynamics and Diagnostics in the Solar Transition Region and Corona (Vol. 446, p. 317).
4. Gopalswamy, N., 2000. Type II solar radio bursts. Series Geophysical Monograph, 119, pp.123-135.
5. Gopalswamy, N., 2011. Coronal mass ejections and solar radio emissions. Planetary, Solar and Heliospheric Radio Emissions (PRE VII), 325pp.
6. Gopalswamy, N., Nitta, N., Akiyama, S., Mäkelä, P. and Yashiro, S., 2012. Coronal magnetic field measurement from EUV images made by the solar dynamics observatory. The Astrophysical Journal, 744(1), p.72, https://doi.org/10.1088/0004-637X/744/1/72.
7. Kishore, P., Ramesh, R., Hariharan, K., Kathiravan, C. and Gopalswamy, N., 2016. Constraining the solar coronal magnetic field strength using split-band type II radio burst observations. The Astrophysical Journal, 832(1), p.59, https://doi.org/10.3847/0004-637X/832/1/59.
8. Klein, K.L., Khan, J.I., Vilmer, N., Delouis, J.M. and Aurass, H., 1999. X-ray and radio evidence on the origin of a coronal shock wave. Astronomy and Astrophysics, v. 346, p. L53-L56 (1999), 346, pp. L53-L56.
9. Kumari, A., Ramesh, R., Kathiravan, C. and Gopalswamy, N., 2017. New evidence for a coronal mass ejection-driven high frequency type II burst near the Sun. The Astrophysical Journal, 843(1), p.10, https://doi.org/10.3847/1538-4357/aa72e7.
10. Kumari, A., Ramesh, R., Kathiravan, C., Wang, T.J. and Gopalswamy, N., 2019. Direct estimates of the solar coronal magnetic field using contemporaneous extreme-ultraviolet, radio, and white-light observations. The Astrophysical Journal, 881(1), p.24, https://doi.org/10.3847/1538-4357/ab2adf.
11. Maxwell, A. and Thompson, A.R., 1962. Spectral Observations of Solar Radio Bursts. II. Slow-Drift Bursts and Coronal Streamers. Astrophysical Journal, vol. 135, p. 138, 135, p.138, https://doi.org/10.1086/147254.
12. Newkirk Jr, G., 1961. The solar corona in active regions and the thermal origin of the slowly varying component of solar radio radiation. Astrophysical Journal, vol. 133, p. 983, 133, p.983.
13. Uchida, Y., 1960. On the exciters of type II and type III solar radio bursts. Publications of the Astronomical Society of Japan, 12(3), pp.376-397, https://doi.org/10.1093/pasj/12.3.376.
14. Umuhire, A.C., Gopalswamy, N., Uwamahoro, J., Akiyama, S., Yashiro, S. and Mäkelä, P., 2021. Properties of high-frequency type II radio bursts and their relation to the associated coronal mass ejections. Solar Physics, 296(1), p.27, https://doi.org/10.1007/s11207-020-01743-8.
15. Vršnak, B., Aurass, H., Magdalenić, J. and Gopalswamy, N., 2001. Band-splitting of coronal and interplanetary type II bursts-I. Basic properties. Astronomy & Astrophysics, 377(1), pp.321-329, https://doi.org/10.1051/0004-6361:20011067.

SAMARQAND DAVLAT UNIVERSITETI ILMIY AXBOROTNOMASI

НАУЧНЫЙ ВЕСТНИК SCIENTIFIC REPORTS

Texnik muharrir **Sh.Xoliqulov**

Muharrirlar:

I.Sulaymonov - fil.f.d., dotsent
E.Arziqulov - f.-m.f.d., dotsent
O.Yusupova - fil.f.n., dotsent

Mas'ul muharrir:

A. Sh. Yarmuxamedov - f.-m.f.n.

Muassis: Samarqand davlat universiteti Manzil: 140104,
Samarqand shahri, Universitet xiyoboni, 15.
Telefon: (0 366) 240-38-47, Faks: (0 366) 239-13-87 e-mail:
axborotnoma.uz
SamDU «Ilmiy axborotnoma» jurnali tahririyati kompyuterida terildi. Bosishga 30.03.2026-yilda ruxsat etildi. Qog'oz o'lchami A-4. Nashriyot hisob tabog'i 10,00
Buyurtma raqami 833. Adadi 30 nusxa.

ISSN 2181-1296